Hindawi
Journal of Optimization
Volume 2018, Article ID 3738049, 12 pages
https://doi.org/10.1155/2018/3738049

Research Article

Jaya Algorithm Guided Procedure to Segment Tumor from Brain MRI

Suresh Chandra Satapathy [1] **and Venkatesan Rajinikanth** [2]

[1] *School of Computer Engineering, Kalinga Institute of Industrial Technology (Deemed to be University), Bhubaneswar 751024, Odisha, India*
[2] *Department of Electronics and Instrumentation Engineering, St. Joseph's College of Engineering, Chennai 600119, India*

Correspondence should be addressed to Venkatesan Rajinikanth; rajinikanthv@stjosephs.ac.in

Received 31 May 2018; Accepted 31 October 2018; Published 14 November 2018

Academic Editor: Wlodzimierz Ogryczak

Brain abnormality is a cause for the chief risk factors in human society with larger morbidity rate. Identification of tumor in its early stage is essential to provide necessary treatment procedure to save the patient. In this work, Jaya Algorithm (JA) and Otsu's Function (OF) guided method is presented to mine the irregular section of brain MRI recorded with Flair and T2 modality. This work implements a two-step process to examine the brain tumor from the axial, sagittal, and coronal views of the two-dimensional (2D) MRI slices. This paper presents a detailed evaluation of thresholding procedure with varied threshold levels (*Th=2,3,4,5*), skull stripping process before/after the thresholding practice, and the tumor extraction based on the Chan-Vese approach. Superiority of JA is confirmed among other prominent heuristic approaches found in literature. The outcome of implemented study confirms that Jaya Algorithm guided method is capable of presenting superior values of Jaccard-Index, Dice-Coefficient, sensitivity, specificity, accuracy, and precision on the BRATS 2015 dataset.

1. Introduction

Image processing procedure plays a vital role in therapeutic data examination [1, 2]. Brain abnormalities such as tumor and stroke are the chief risk factors in human society which affects the people irrespective of their gender and geographical location. Usually, the severity and the cause for the brain abnormalities are diagnosed in medical clinics based on a predefined procedures constructed by experienced doctors. This procedures involves in the recording the signals and the images of brain under a controlled environment. After recording the essential information from the patient, a prescreening procedure is to be executed using the manual or automated procedures to assess the cause and the harshness of the severity. After the prescreening process, a prescribed clinical evaluation procedure is then executed with the patient in order to arrange for further handling procedure to control and cure the abnormalities [3].

Normally, the condition of the brain can be evaluated based on a single-channel and multichannel EEG signals recorded using the external electrodes or the brain images recorded with MRI and CT imaging approaches [4–7]. Previous study confirms that information existing in brain image is essential to categorize and localize the abnormality compared to the brain signals [8]. If needed, a mapping of brain signal and image can also be carried to locate the cause and region of the brain abnormality.

In literature, a considerable amount of conventional and soft-computing guided measures are widely employed to examine the brain pictures recorded with MRI and CT [9, 10]. The information available in MRI is better compared to CT because of its multimodality, since the MRI supports a range of modalities, like Flair, T1, T1C, T2, and DW [11–14]. The visibility of the abnormality in Flair and T2 modality is superior to other approaches. Hence, in this paper, the brain images recorded with the Flair and T2 are used for the examination.

This work implements a two-stage scheme to mine and appraise the tumor using the Jaya Algorithm (JA) and Otsu's Function (OF) based thresholding and the Chan-Vese

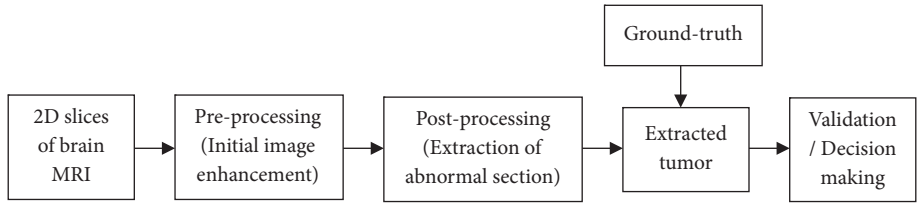

Figure 1: Stages in the proposed brain MRI examination scheme.

(CV) based segmentation procedure to extract the abnormal section from the two-dimension (2D) slices of the brain MRI. The performance of JA is confirmed against other heuristic algorithms existing in the literature. Correctness of the proposed approach is also confirmed by computing the image likeliness measures based on a comparative study linking the mined tumor section and the ground-truth (GT) image. The experimental results of this work confirm that the JA assisted procedure tenders improved result on the 2D brain slices recorded with Flair and T2 modalities.

2. Related Previous Works

In brain imaging literature, a significant number of conventional and soft-computing (SC) based techniques are discussed and executed to extract and evaluate the brain abnormality. The earlier works also suggests that traditional approaches may implement a single-step or two-step procedure to extract the abnormal section from the chosen MRI slice [11, 15, 16]. Most of these procedures are modality specific and works well only for few modality cases, such as Flair and T2. To overcome these limitations, heuristic algorithm assisted two-step events are broadly adopted to examine the brain abnormality recorded using MRI of various modalities. Palani et al. (2016) implemented a SC approach to segment the soft brain tissues using a two-step procedure based on Otsu's thresholding [8]. Chaddad (2015) implemented Gaussian mixture model technique to support automated feature extraction in brain tumor extracted from MRI [17]. Dey et al. (2015) applied genetic algorithm tuned interval filter to remove noise in brain MRI [6]. Rajinikanth and Satapathy (2018) implemented a detailed evaluation of the brain MRI with various segmentation approaches [9]. The works of Rajinikanth et al. (2017) also implemented various heuristic evaluation procedures to separate the abnormal area from brain MRI recorded with a range of modalities [18]. The work of Rajinikanth et al. (2018) also confirmed that the need for image fusion methods to enhance the accuracy in brain MRI evaluation [13]. Recently, Amin et al. (2017; 2018) proposed a distinctive approach as well as the deep-learning procedure to extract the abnormal sections from the brain MRI [4, 5]. Every machine-learning and deep-learning method in the literature discuss about their own merit and demerits. The brain MRI examination procedure always needs efficient as well as reliable procedures to mine and evaluate the strange segment from the brain picture [19].

Researchers have already implemented a considerable number of swarm-based/evolutionary approaches to examine the brain MRI [9, 13]. This paper attempts a methodology to implement the recently developed approach called the Jaya Algorithm (JA). The literature also confirms that implementation of JA is quite simple contrast to former heuristic schemes [20–23]. Further, this paper implements the Chan-Vese method to mine the tumor section in preprocessed picture. Finally, the superiority of executed approach is confirmed using a qualified investigation among the extracted tumor section and the GT picture [9].

3. Materials and Methods

This division of the manuscript provides the details of the two-step procedure employed to inspect the abnormality of brain MRI. This section presents the summary of the pre- and postprocessing methods implemented to examine the test pictures of 2D brain MRI.

Figure 1 shows the stages involved in the proposed work. This technique initially considers a 2D MRI slice as the test pictures to be processed. The preprocessing stage enhances the abnormal region of the test picture by implementing a multithresholding scheme with or without the skull section. Recent work of Rajinikanth and Satapathy (2018) discussed that skull-elimination is essential to implement fully automated disease examination schemes [9]. The outcome of the initial stage is then processed by the postprocessing stage, which implements a chosen image separation method to extort the abnormal section. The performance of MRI examination method is then established by a relative analysis among extracted tumor section and GT picture. Final result of this scheme is then considered to support the decision making and treatment planning procedure.

3.1. Preprocessing Stage. It is the initial step in the two-stage process. This implements a multithresholding process to enhance the tumor section of 2D test picture. This stage implements the Jaya Algorithm (JA) assisted Otsu's between-class variance procedure for different threshold (Th) levels ($Th = 2,3,4,5$) on the chosen test image. Later, the image quality metrics are computed for these images to discover the best threshold for the image enhancement.

3.1.1. JAYA Algorithm. JA is a newly invented evolutionary algorithm by Rao (2016) [20] and its theory and the working principle can be found in [21–23]. The chief merit of the JA compared with other considered heuristic/evolutionary approaches, such as the Firefly Algorithm (FA), Teaching-Learning Based Optimization (TLBO), Particle-Swarm-Optimization (PSO), Bacterial-Optimization (BFO),

and Bat-Algorithm (BA), involves minimal early parameters to be assigned [2, 12–14, 19, 24–27].

Let $G(x)_{max}$ is the preferred objective function, $\Re 1 = \Re 2$ are subjective quantities of option [0,1], N is population amount (i.e., $n=1,2,\ldots,N$), and i and D indicates the amount of iterations and dimensions (i.e., $j=1,2,\ldots,D$) correspondingly.

At some occurrence in the algorithm, $G(x)_{best}$ and $G(x)_{worst}$ signify the finest and worst results reached through the contestant in population.

The prime equation of JA is presented below:

$$X^1{}_{j,n,i} = X_{j,n,i} + \Re 1_{j,i}\left(X_{jbest,i} - \left|X_{j,n,i}\right|\right) - \Re 2_{j,i}\left(X_{jworst,i} - \left|X_{j,n,i}\right|\right) \tag{1}$$

where $X_{j,n,i}$ signify the j^{th} variable of n^{th} contestant at i^{th} iteration and $X^1{}_{j,n,i}$ indicate the modernized value. In this work, JA is utilized to discover the maximized value of the Otsu's between-class variance value for a chosen '*Th*'.

Additional details concerning the conventional JA and its recent advancements can be found in recent literature [28–35].

3.1.2. Otsu's Function. From the year 1979, Otsu's thresholding is broadly considered to enhance the traditional and medical images [36]. The theory of Otsu is as follows: for multithresholding problem (*Th=2,3,4,5*), input image is separated into various groups from H_0 and H_{Th-1} based on the chosen Th. The class H_0 encloses the gray levels in the range 0 to t-1 and class H_{Th-1} encircles the gray levels from t to L – 1. The probability distributions for gray levels H_0 and HTh_{-1} can be articulated as [37, 38]

$$H_0 = \frac{p_0}{\omega_0(t)} \cdots \frac{p_{t-1}}{\omega_0(t)}, \ldots, H_{Th\text{-}1} = \frac{p_t}{\omega_{Th\text{-}1}(t)} \cdots \frac{p_{L-1}}{\omega_{Th\text{-}1}(t)} \tag{2}$$

where $\omega_0(t) = \sum_{i=0}^{t-1} p_i, \ldots, \omega_{Th-1}(t) = \sum_{i=t}^{L-1} p_i$ and L=256.

The mean levels $m_0, \ldots, m_{Th-1}$ for $H_0, \ldots, H_{Th\text{-}1}$ can be articulated as

$$m_0 = \sum_{i=0}^{t-1} \frac{ip_i}{\omega_0(t)}, \ldots, m_{Th-1} = \sum_{i=t}^{L-1} \frac{ip_i}{\omega_{Th-1}(t)} \tag{3}$$

The mean intensity (m_T) of total picture can be represented as

$$m_T = \omega_0 m_0 + \ldots + \omega_{Th-1} m_{Th-1}, \quad \omega_0 + \ldots + \omega_{Th-1} = 1 \tag{4}$$

The objective function for the bilevel thresholding problem can be expressed as

$$\text{Maximize} \quad J(Th) = \sigma_0 + \ldots + \sigma_{Th\text{-}1} \tag{5}$$

where $\sigma_0 = \omega_0(m_0 - m_T)^2, \ldots, \sigma_{Th\text{-}1} = \omega_{Th\text{-}1}(\mu_{Th\text{-}1} - \mu_T)^2$.

Additional details regarding Otsu can be found from [24, 25, 39–41].

3.1.3. Realization. During the realization of the preprocessing stage, the initial JA factors are allotted as follows: agents size (N) = 20, number of iterations=2000, dimension of explore (D) =*Th*, and the stopping criterion if the maximized Otsu's value.

Initially, the 2D slices of Cerebrix and Brainix images of size 256x256 pixels are considered for the examination [42]. These images are associated with the skull section. Hence, the proposed paper implements the skull-elimination procedure under the following conditions: (i) skull stripping before the thresholding and (ii) skull stripping after the thresholding. Similarly, in order to confirm the best threshold during the initial picture processing, various thresholds are chosen (*Th=2,3,4,5*) and the superiority of the outcome is assessed using the image quality measure values, such as RMSE, PSNR, SSIM, NCC, AD, and SC (Satapathy et al. 2018); further, the CPU runtime in seconds also recorded to choose the threshold level in order to get the better throughput during the image analysis. The thresholding procedure is initially implemented with JA+Otsu. Later, other heuristic approaches are considered to validate the superiority of JA compared to the chosen heuristic procedures. Finally, the abnormal section of the brain MRI is extracted using the Chan-Vese segmentation procedure.

3.2. Postprocessing. This section implements the Chan-Vese (CV) active-contour practice to mine the irregular section from preprocessed MRI [9]. CV is a bounding box based semiautomated technique implemented by Chan and Vese to extract the information from the test pictures [9]. Recently, CV is widely adopted to extract the chosen regions of medicinal image under assessment [43–45]. The working of CV is similar to the level-set procedure, in which the edges of the box are corrected incessantly based on the allocated iteration quantity. If grouping of pixel inside the box is over, the area within the contour will be extracted and displayed. In this work, CV is utilized to mine the irregular section (tumor) from preprocessed brain MRI of Flair and T2 modality [15, 46].

3.3. Evaluation. The major aim of this paper is to extract tumor in the 2D brain MRI and to compute the features of tumor region for further study. In this work, two kinds of data, such as brain MRI with and without the ground truth (GT), are considered. Image likeness values, such as Jaccard-Index (JI), Dice-Coefficient (DC), False-Positive-Rate (FPR), and False-Negative-Rate (FNR), are computed for MRI with GT [2, 9, 47].

The arithmetic expression is shown below:

$$JI(IGT, IO) = \frac{IGT \cap IO}{IGT \cup IO} \tag{6}$$

$$DC(IGT, IO) = \frac{2(IGT \cap IO)}{|IGT| \cup |IO|} \tag{7}$$

$$FPR(IGT, IO) = \frac{(IGT/IO)}{(IGT \cup IO)} \tag{8}$$

$$FNR\,(IGT, IO) = \frac{(IO/IGT)}{(IGT \cup IO)} \tag{9}$$

where IGT symbolize the GT and IO symbolize mined region.

Further, values, like sensitivity (SE), specificity (SP), accuracy (AC), precision (PR), Balanced-Classification-Rate (BCR), and Balanced-Error-Rate (BER), are measured. Mathematical expression for these parameters is given below:

$$SE = \frac{T_P}{(T_P + F_N)} \tag{10}$$

$$SP = \frac{T_N}{(T_N + F_P)} \tag{11}$$

$$AC = \frac{(T_P + T_N)}{(T_P + T_N + F_P + F_N)} \tag{12}$$

$$PR = \frac{T_P}{(T_P + F_P)} \tag{13}$$

$$BCR = \frac{1}{2\,(T_P/\,(T_P + F_N) + T_N/\,(T_N + F_P))} \tag{14}$$

$$BER = 1 - BCR \tag{15}$$

where T_N, T_P, F_N, and F_P indicates true-negative, true-positive, false-negative, and false-positive, correspondingly.

4. Results and Discussion

This division of the paper presents the investigational outcome of the proposed methodology using the brain MRI of Brainix (256x256 pixels), Cerebrix (256x256 pixels), and BRATS 2015 (216x160 pixels) database [48]. The work is executed in Matlab7 using a system; AMD C70 Dual Core 1 GHz CPU with 4 GB of RAM. The work implemented in this paper is as follows: (i) selecting the 2D brain MRI slices, (ii) implementation of skull stripping procedure, (iii) thresholding based enhancement with JA+Otsu, (iv) extraction of the tumor using CV, and (v) computation of picture similarity values to validate the implemented procedure.

Initially, the chosen test images of Brainix dataset is considered for the evaluation, and the various modality based 2D slices of this dataset is depicted in Figure 2. Later, a skull-elimination procedure discussed by Rajinikanth et al. (2017) is implemented for this test pictures and its outcome is presented in Figure 3 [18].

Figures 3(a) and 3(c) show the skull stripped soft brain regions and Figures 3(b) and 3(d) show the stripped skull section. The gray histogram of Flair modality image of Figure 2(a) is presented in Figure 4. Figure 4(a) shows the histogram with the skull section and Figure 4(b) shows the histogram without the skull. From these images, it can be observed that the peak histogram distribution is approximately similar in both the cases. This confirms that the multithresholding result will be approximately similar for both the image cases. From this, it is clear that the skull region will not affect the quality of the multithresholding output of the brain MRIs. Similar results are obtained for other cases, such as T1 and T2 modalities. The visibility of tumor in T1 modality is poor, hence in this paper only the Flair and T2 modality MRIs are considered for the evaluation.

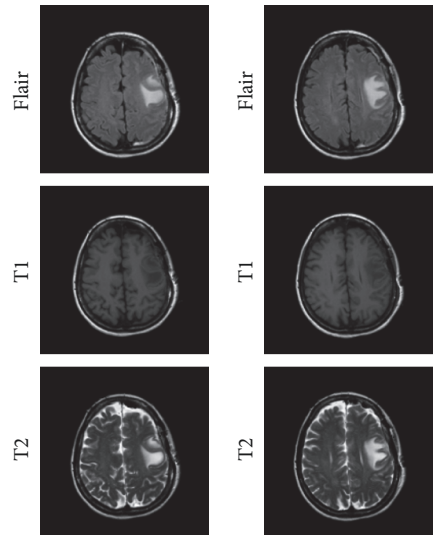

(a) Slice1 (b) Slice2

Figure 2: Axial view brain MRI of size 256x256 pixels.

Initially, in order to know the best threshold level for the preprocessing of the image, the JA+Otsu based approach is implemented with various threshold values, like Th=2,3,4,5 and the equivalent outcomes are described in Figure 5. It confirms that the skull stripping task can also be implemented after the thresholding task. To decide the best threshold level for the MRI, the image similarity values are calculated based on a relative analysis among the original test image and the thresholded image, and its outcomes are described in Table 1. When Th=2, the visibility of tumor section in the preprocessed image is very poor. When threshold level increases, the image quality measure as well as the CPU run time increases. From this study, it can be noted that Th=3 tender enhanced thresholding outcome with minimised CPU time compared with Th=4 and 5. Hence, in this paper, trilevel threshold is chosen to preprocess the test pictures considered in this study.

The thresholding performance of the JA algorithm is then tested against other heuristic/evolutionary approaches, such as FA, TLBO, PSO, BFO, and BA and the convergence of this optimization search for Th=2 (axial view Flair MRI) is presented in Figure 6. This result confirms that the average CPU time taken by the JA is lesser compared to the BFO and PSO algorithms for the chosen test image. The FA, TLBO, and BA offer better CPU time for the chosen images, but the number of initial parameters to be assigned in JA is smaller than these approaches. This result confirms that JA can be chosen to preprocess the brain MRI compared to the alternative approaches chosen in this paper.

After implementing the preprocessing with JA+Otsu, the CV segmentation procedure is then implemented to extract the tumor section from the axial view brain MRI. Figure 7 shows the outcome of the postprocessing section obtained

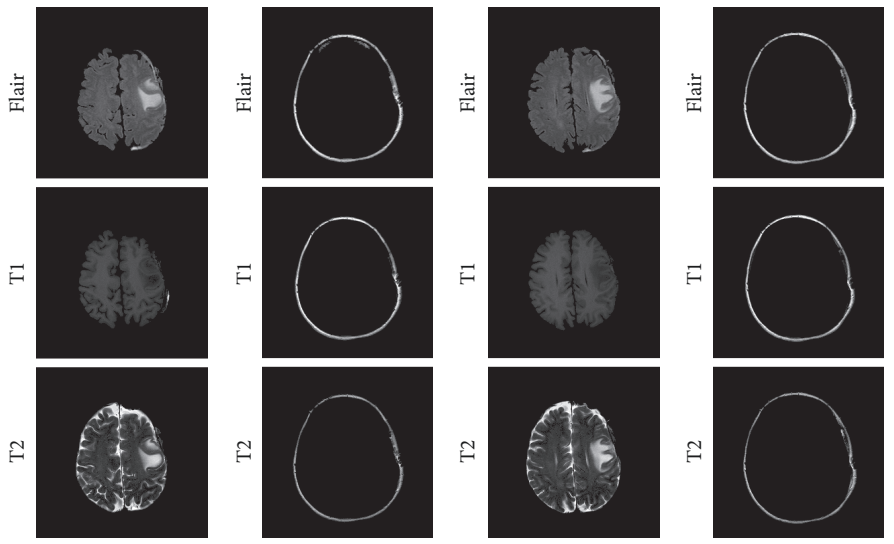

(a) Slice1 (b) Skull of Slice1 (c) Slice2 (d) Skull of Slice2

Figure 3: Skull eliminated brain MRI.

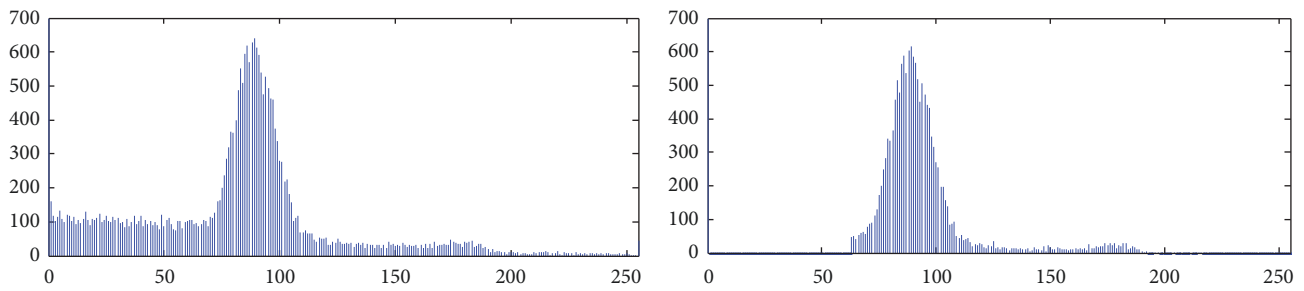

(a) Histogram with skull (b) Histogram without skull

Figure 4: Gray histogram of a chosen test image (Flair) with and without skull section.

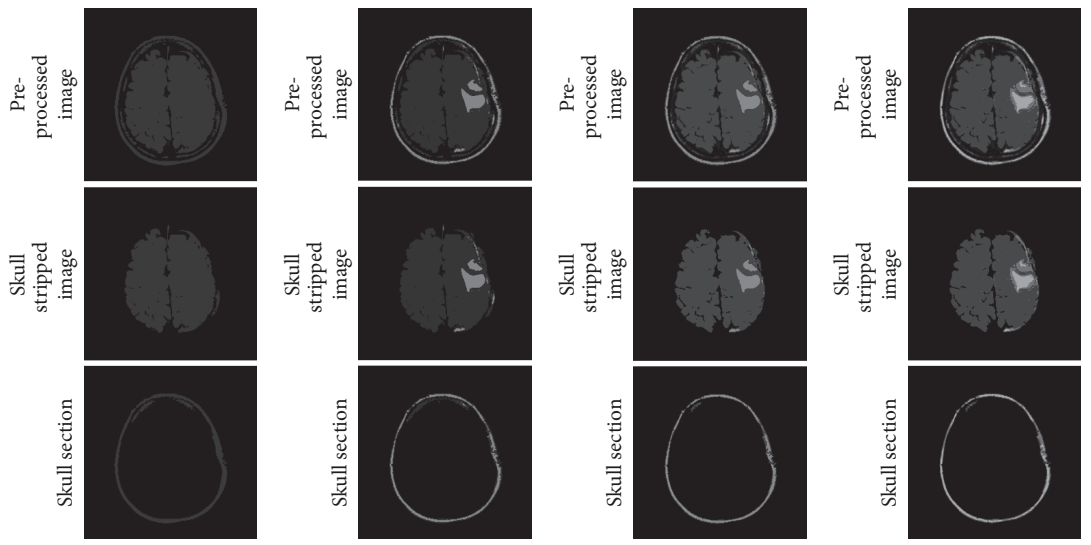

(a) Th=2 (b) Th=3 (c) Th=4 (d) Th=5

Figure 5: Skull section removal after the multithresholding.

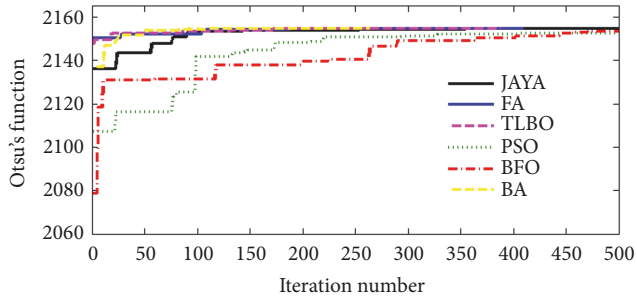

Figure 6: Convergence of heuristic search (*Th*=2).

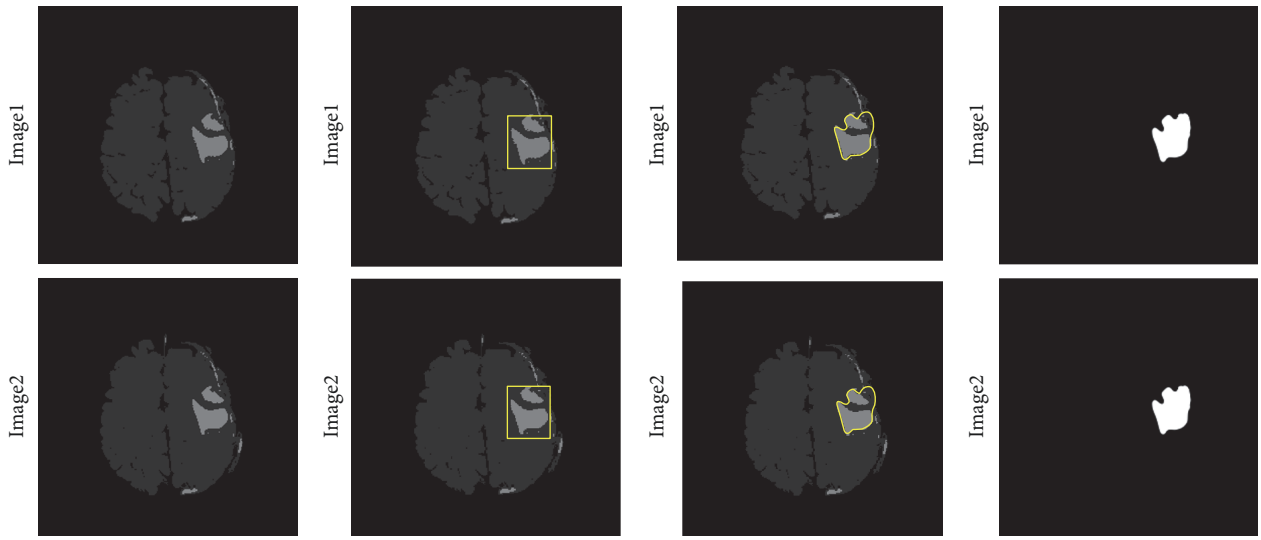

(a) Preprocessed image (b) Initial bounding box (c) Final CV (d) Extracted tumor

Figure 7: Results of CV based segmentation.

with a sample test picture. As shown in Figure 7(b), initially a bounding box over the tumor region is assigned manually. When the Chan-Vese approach is executed, the bounding box will shrink toward the inner region in order to identify all the possible pixel values of the tumor section. This shrinking process will be executed based on the assigned iteration value, after completing the iteration; the pixel region bounded by the CV contour is extracted and is presented as the tumor section. Figure 7(c) depicts the final contour of the CV and Figure 7(d) shows the extracted tumor section. Similar procedure is implemented for other test images considered in this paper. Further, the segmentation performance of the CV is also confirmed against active-contour (AC) and Region Growing (RG) techniques existing in the literature.

Figure 8 shows the sample images of coronal and sagittal views of Cerebrix dataset. When compared with the axial view, skull stripping and the tumor extraction are quite difficult in these views due to its image complexity. Recent works confirm that an efficient skull-elimination procedure will help to overcome this difficulty [9]. Initially, the skull-elimination is implemented to separate the soft brain section from the high intensity skull using the procedure discussed in [15]. Later, the preprocessing and the postprocessing approaches are implemented for these images in order to extract the tumor section.

Figure 9 presents the outcome of the proposed technique with the sample Cerebrix MRIs. Figure 9(a) presents the preprocessed test picture and Figures 9(b), 9(c), and 9(d) show the extracted tumor sections with CV, AC, and RG, respectively. The Cerebrix dataset does not have the ground-truth (GT) image. Hence, in order to validate the performance of proposed approach, grand challenge benchmark image dataset called the BRATS2015 dataset is considered.

The main advantage of the BRATS2015 dataset compared to the Brainix and Cerebrix is as follows: (i) it has a skull stripped 3D brain MRI from which the required amount of 2D slices can be extracted, (ii) it supports the modalities, such as Flair, T1, T1C, and T2, and (iii) it has a common GT picture offered by an expert member. Due to this reason, BRATS images are widely adopted by most of the researchers to test their disease examination tool [11].

Figure 10 shows the sample test images of axial view MRI recorded with various modalities and its corresponding GT. In this paper, the Flair and T2 modality images are considered for the study. Figure 11 shows the JA+Otsu based trilevel thresholding result for the chosen BRATS dataset and also

Table 1: Image quality measures for the chosen test image (Flair) for various *Th* values.

Test image	RMSE	PSNR	SSIM	NCC	AD	SC	CPU time
Threshold2	32.6324	17.8578	0.7674	0.4546	16.0188	4.2512	24.6264
Threshold3	25.9206	19.8579	0.8097	0.5777	14.1803	2.7689	31.3827
Threshold4	17.3467	23.3465	0.8798	0.7241	8.7682	1.8508	58.8926
Threshold5	14.9659	24.6288	0.8912	0.7688	7.9169	1.6496	73.3028

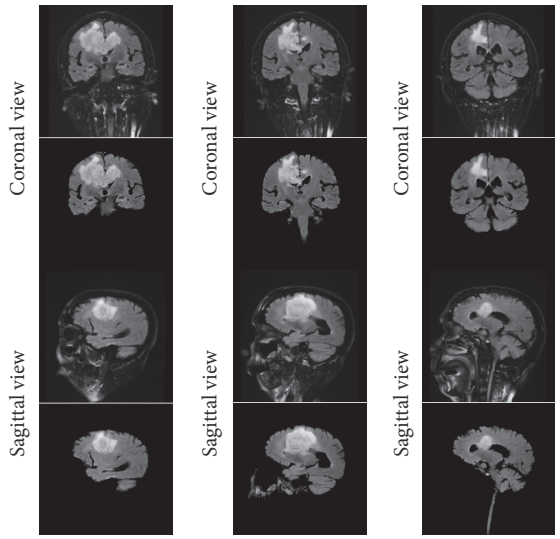

(a) Slice1 (b) Slice2 (c) Slice3

Figure 8: Chosen test images of coronal and sagittal view MRIs.

the segmentation results. Figure 11(a) shows the slice number, Figures 11(b) and 11(d) depict the preprocessed picture and Figures 11(c) and 11(e) show the extracted tumor region with CV technique.

Later, the superiority of implemented procedure is confirmed using a comparative study between the extracted tumor section and the GT, and the essential image similarity values and statistical values are computed for both the Flair and T2 modality cases. Tables 2 and 3 show the results obtained with the Flair modality test pictures. Similar results are attained for the T2 modality images. These tables confirm that proposed technique is efficient in attaining better values of JI, DC, sensitivity, specificity, accuracy, and precision compared with the segmentation procedures, like AC and RG considered in this study.

The overall performance (average of the image quality measures obtained for the trilevel thresholding) of the algorithms considered in this paper is depicted in Figure 12 and it confirms that the optimization performance of the JA is superior to other methods considered in this paper. In Figure 12, the x-axis numbers 1 to 6 denote the soft-computing methods, like JA, FA, TLBO, PSO, BFO, and BA correspondingly.

The main limitation of the proposed procedure is as follows: it is a semiautomated approach and requires the assistance of the operator to fix the threshold value during the preprocessing task and also requires the operators assistance during the bounding box initiation while implementing the CV segmentation. In future, the tumor segmentation and evaluation procedure can be automated by implementing the recent procedure known deep-learning approach. But, the complexity in training the required task is more compared to the approach discussed in this paper. The results of this paper confirm that proposed approach is very efficient in extracting the tumor section from various datasets considered in this paper. This paper also confirms that this approach works well on Flair and T2 modality MRIs.

In future, a feature extraction and classification procedure for the extracted tumor section can be implemented to classify the brain tumors, such as benign, and malignant. Further, the adopted brain MRI images can be examined using the deep-learning procedures based on the Neural Network (NN) [49–51] and its outcome can be compared and validated with the machine-learning procedure discussed in this work.

5. Conclusions

This paper implements the combination of a preprocessing and a postprocessing to mine the irregular section of the brain MRI. The preprocessing is implemented to enhance the tumor section using a multithresholding based on the Jaya Algorithm and Otsu's function and the postprocessing implements the Chan-Vese (CV) segmentation procedure

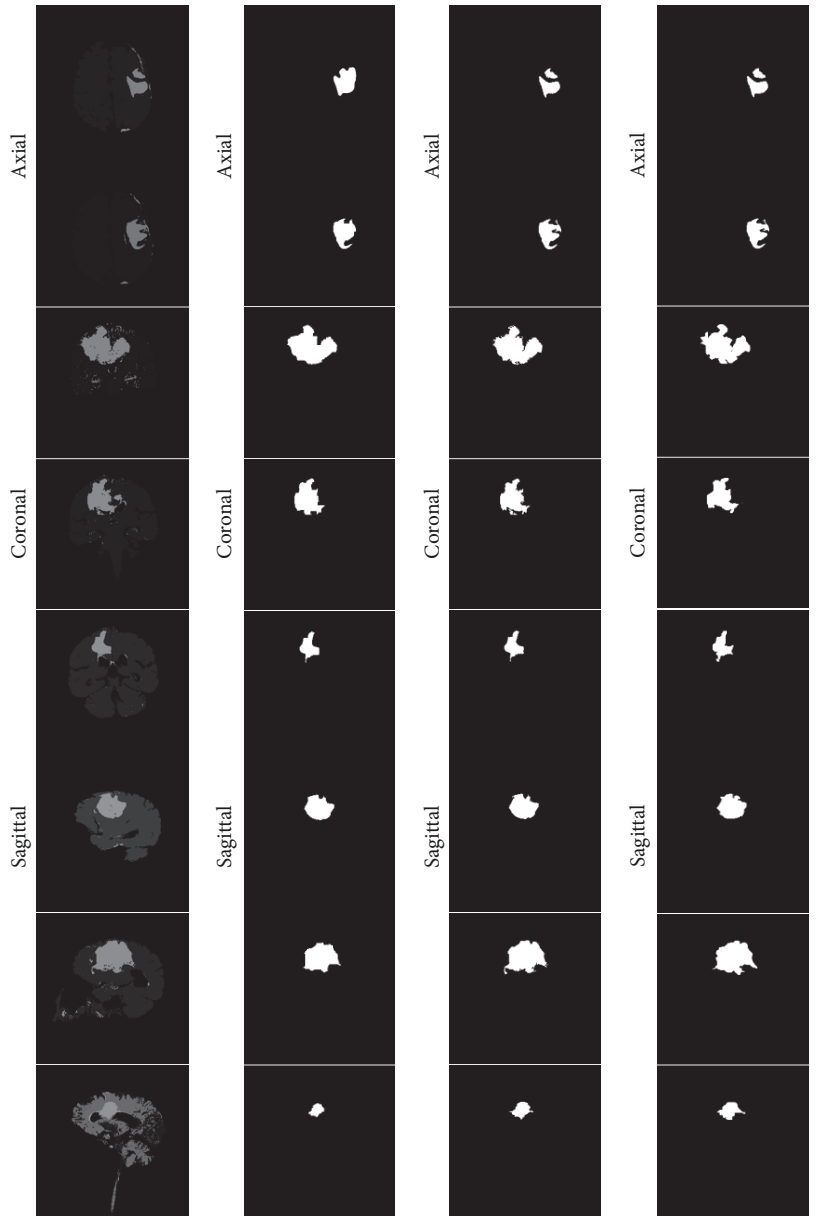

(a) Test picture (b) CV (c) AC (d) RG

Figure 9: Segmented tumor section with CV, AC, and RG.

Table 2: Picture likeness measures obtained for the flair modality images.

Image	TPR	TNR	FPR	FNR	JI	DC
F100	0.8196	0.9946	0.0054	0.1804	0.7628	0.8655
F110	0.9132	0.9933	0.0067	0.0868	0.8376	0.9116
F120	0.9072	0.9921	0.0079	0.0928	0.8187	0.9003
F130	0.8446	0.9926	0.0074	0.1554	0.7357	0.8477
T2100	0.7533	0.9953	0.0047	0.2467	0.7071	0.8284
T2110	0.9006	0.9936	0.0064	0.0994	0.8293	0.9067
T2120	0.8433	0.9921	0.0079	0.1567	0.7610	0.8643
T2130	0.8114	0.9930	0.0070	0.1886	0.7127	0.8322
Average	0.8492	0.9933	0.0067	0.1508	0.7706	0.8696

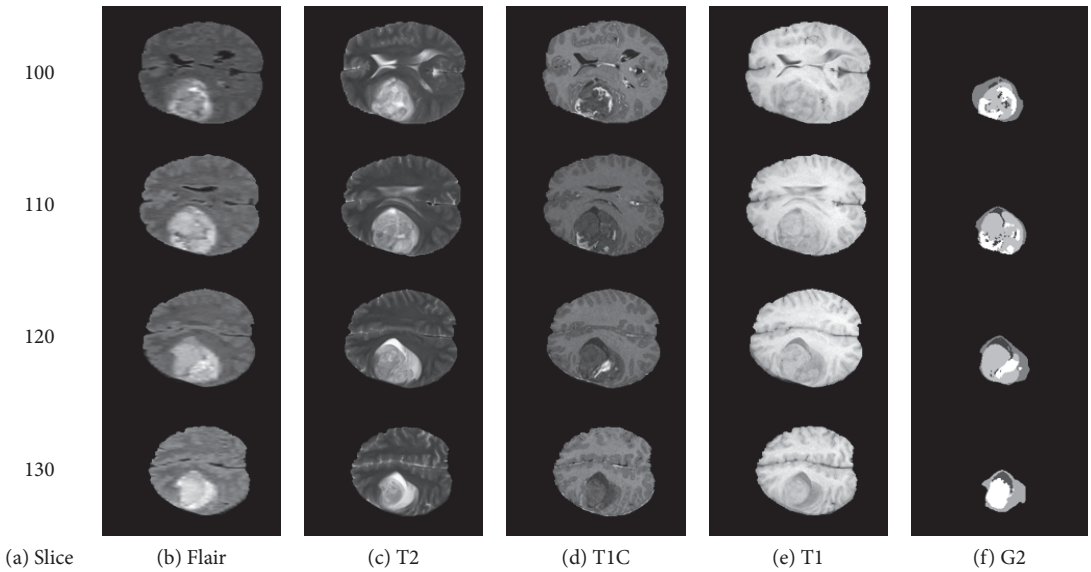

Figure 10: Sample test images of BRATS2015.

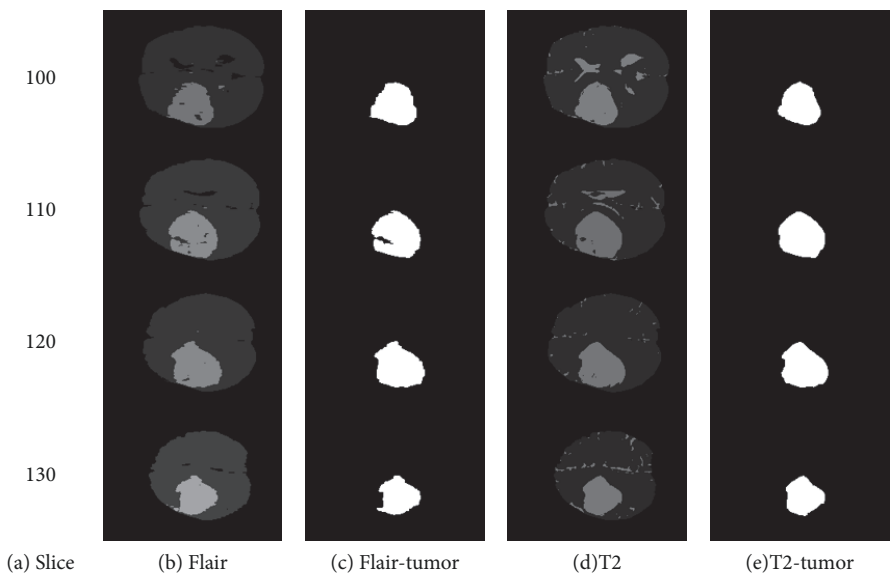

Figure 11: Segmentation results obtained for BRATS2015 dataset.

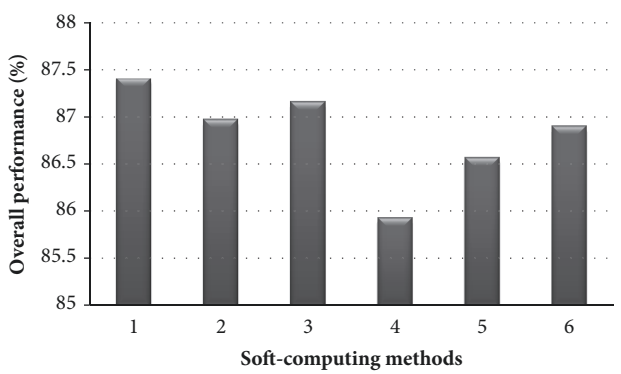

Figure 12: Performance evaluation of considered heuristic algorithms.

Table 3: Picture statistical measures obtained for the flair modality images.

Image	Sensitivity	Specificity	Accuracy	Precision
F100	0.8196	0.9946	0.9829	0.9167
F110	0.9132	0.9933	0.9877	0.9101
F120	0.9072	0.9921	0.9863	0.8935
F130	0.8446	0.9926	0.9855	0.8508
T2100	0.7533	0.9953	0.9790	0.9201
T2110	0.9006	0.9936	0.9872	0.9128
T2120	0.8433	0.9921	0.9820	0.8864
T2130	0.8114	0.9930	0.9843	0.8542
Average	0.8492	0.9933	0.9844	0.8931

to extract the tumor. During this work, the brain MRI images are obtained from the benchmark datasets, such as Brainix, Cerebrix and BRATS2015. Initially, an excrement is implemented to recognize the best threshold value for the chosen problem, and the results of the preprocessing confirm that the trilevel thresholding offers better result for the brain tumor evaluation for both the Flair and T2 modalities. Later, the performance of CV is compared against the AC and RG procedures. The segmentation result confirms that CV offers better result compared to AC and RG. Finally, the overall performance of the proposed approach is tested and confirmed with the BRATS2015 brain MRI database. The investigational outcome of this study substantiates that JA+Otsu and CV based procedure offer improved picture excellence measures, image likeness measures, and image statistical measures for the considered dataset. In future, CV segmentation can be validated against other segmentation procedures existing in the medical imaging literature.

Data Availability

Previously reported Brain MRI data were used to support this study and are available at http://www.osirix-viewer.com/datasets/ and http://hal.inria.fr/hal-00935640. These prior studies and datasets are cited at relevant places within the text as [11, 42, 48].

Conflicts of Interest

The authors declare that there are no conflicts of interest regarding the publication of this paper.

References

[1] A. Pillai, R. Soundrapandiyan, S. Satapathy, S. C. Satapathy, K.-H. Jung, and R. Krishnan, "Local diagonal extrema number pattern: A new feature descriptor for face recognition," *Future Generation Computer Systems*, vol. 81, pp. 297–306, 2018.

[2] N. S. M. Raja, V. Rajinikanth, S. L. Fernandes, and S. C. Satapathy, "Segmentation of breast thermal images using kapur's entropy and hidden markov random field," *Journal of Medical Imaging and Health Informatics*, vol. 7, no. 8, pp. 1825–1829, 2017.

[3] V. Bhateja, M. Misra, and S. Urooj, "Unsharp masking approaches for HVS based enhancement of mammographic masses: A comparative evaluation," *Future Generation Computer Systems*, vol. 82, pp. 176–189, 2018.

[4] J. Amin, M. Sharif, M. Yasmin, and S. L. Fernandes, "A distinctive approach in brain tumor detection and classification using MRI," *Pattern Recognition Letters*, 2017.

[5] J. Amin, M. Sharif, M. Yasmin, and S. L. Fernandes, "Big data analysis for brain tumor detection: Deep convolutional neural networks," *Future Generation Computer Systems*, vol. 87, pp. 290–297, 2018.

[6] N. Dey, A. Ashour, S. Beagum et al., "Parameter optimization for local polynomial approximation based intersection confidence interval filter using genetic algorithm: an application for brain MRI image de-noising," *Journal of Imaging*, vol. 1, no. 1, pp. 60–84, 2015.

[7] S. L. Fernandes, V. P. Gurupur, H. Lin, and R. J. Martis, "A novel fusion approach for early lung cancer detection using computer aided diagnosis techniques," *Journal of Medical Imaging and Health Informatics*, vol. 7, no. 8, pp. 1841–1850, 2017.

[8] P. T. Krishnan, P. Balasubramanian, and C. Krishnan, "Segmentation of brain regions by integrating meta heuristic multilevel threshold with markov random field," *Current Medical Imaging Reviews*, vol. 12, no. 1, pp. 4–12, 2016.

[9] V. Rajinikanth and S. C. Satapathy, "Segmentation of Ischemic stroke lesion in brain mri based on social group optimization and fuzzy-Tsallis entropy," *Arabian Journal for Science and Engineering*, vol. 43, no. 8, pp. 4365–4378, 2018.

[10] V. Rajinikanth, S. C. Satapathy, N. Dey, and R. Vijayarajan, "DWT-PCA image fusion technique to improve segmentation accuracy in brain tumor analysis," *Lecture Notes in Electrical Engineering*, vol. 471, pp. 453–462, 2018.

[11] Menze, "The multimodal brain tumor image segmentation benchmark (BRATS)," *IEEE T Med Imaging*, vol. 34, no. 10, pp. 1993–2024, 2015.

[12] N. S. Raja, S. L. Fernandes, N. Dey, S. C. Satapathy, and V. Rajinikanth, "Contrast enhanced medical MRI evaluation using Tsallis entropy and region growing segmentation," *Journal of Ambient Intelligence and Humanized Computing*, pp. 1–12, 2018.

[13] V. Rajinikanth, N. Dey, S. C. Satapathy, and A. S. Ashour, "An approach to examine Magnetic Resonance Angiography based on Tsallis entropy and deformable snake model," *Future Generation Computer Systems*, vol. 85, pp. 160–172, 2018.

[14] V. Rajinikanth, S. L. Fernandes, B. Bhushan, Harisha, and N. R. Sunder, "Segmentation and analysis of brain tumor using tsallis entropy and regularised level set," *Lecture Notes in Electrical Engineering*, vol. 434, pp. 313–321, 2018.

[15] I. T. Roopini, M. Vasanthi, V. Rajinikanth, M. Rekha, and M. Sangeetha, "Segmentation of tumor from brain MRI using fuzzy

entropy and distance regularised level set," in *Computational Signal Processing and Analysis*, vol. 490 of *Lecture Notes in Electrical Engineering*, pp. 297–304, Springer, Singapore, 2018.

[16] A. Srivastava, V. Bhateja, H. Tiwari, and S. C. Satapathy, "Restoration algorithm for gaussian corrupted MRI using non-local averaging," in *Information Systems Design and Intelligent Applications*, vol. 340 of *Advances in Intelligent Systems and Computing*, pp. 831–840, Springer India, New Delhi, 2015.

[17] A. Chaddad, "Automated feature extraction in brain tumor by magnetic resonance imaging using gaussian mixture models," *International Journal of Biomedical Imaging*, vol. 2015, Article ID 868031, 11 pages, 2015.

[18] V. Rajinikanth, N. S. M. Raja, and K. Kamalanand, "Firefly algorithm assisted segmentation of tumor from brain MRI using Tsallis function and Markov Random Field," *Control Engineering and Applied Informatics*, vol. 19, no. 3, pp. 97–106, 2017.

[19] Y. Xin-She, *Nature-Inspired Metaheuristic Algorithms*, Luniver Press, Frome, 2nd edition, 2008.

[20] R. V. Rao, "Jaya: a simple and new optimization algorithm for solving constrained and unconstrained optimization problems," *International Journal of Industrial Engineering Computations*, vol. 7, no. 1, pp. 19–34, 2016.

[21] R. Rao and K. More, "Design optimization and analysis of selected thermal devices using self-adaptive Jaya algorithm," *Energy Conversion and Management*, vol. 140, pp. 24–35, 2017.

[22] R. V. Rao and A. Saroj, "A self-adaptive multi-population based Jaya algorithm for engineering optimization," *Swarm and Evolutionary Computation*, vol. 37, pp. 1–26, 2017.

[23] R. V. Rao and A. Saroj, "Constrained economic optimization of shell-and-tube heat exchangers using elitist-Jaya algorithm," *Energy*, vol. 128, pp. 785–800, 2017.

[24] N. S. M. Raja, V. Rajinikanth, and K. Latha, "Otsu based optimal multilevel image thresholding using firefly algorithm," *Modelling and Simulation in Engineering*, vol. 2014, Article ID 794574, 17 pages, 2014.

[25] V. Rajinikanth and M. S. Couceiro, "Optimal multilevel image threshold selection using a novel objective function," in *Information Systems Design and Intelligent Applications*, vol. 340 of *Advances in Intelligent Systems and Computing*, pp. 177–186, Springer India, New Delhi, 2015.

[26] Y. Xin-She and H. Xingshi, "Bat algorithm: literature review and applications," *International Journal of Bio-Inspired Computation*, vol. 5, no. 3, pp. 141–149, 2013.

[27] X.-S. Yang and A. H. Gandomi, "Bat algorithm: A novel approach for global engineering optimization," *Engineering Computations*, vol. 29, no. 5, pp. 464–483, 2012.

[28] R. V. Rao, "Jaya optimization algorithm and its variants," in *Jaya: An Advanced Optimization Algorithm and its Engineering Applications*, Springer, Cham, 2019.

[29] R. V. Rao, D. P. Rai, and J. Balic, "Optimization of abrasive water-jet machining process using multi-objective jaya algorithm," *Materials Today: Proceedings*, vol. 5, no. 2, pp. 4930–4938, 2018.

[30] R. V. Rao and H. S. Keesari, "Multi-team perturbation guiding Jaya algorithm for optimization of wind farm layout," *Applied Soft Computing*, vol. 71, pp. 800–815, 2018.

[31] R. V. Rao, A. Saroj, P. Ocloń, J. Taler, and D. Taler, "Single- and Multi-Objective Design Optimization of Plate-Fin Heat Exchangers Using Jaya Algorithm," *Heat Transfer Engineering*, vol. 39, no. 13-14, pp. 1201–1216, 2017.

[32] R. V. Rao and A. Saroj, "An elitism-based self-adaptive multi-population Jaya algorithm and its applications," *Soft Computing*, pp. 1–24, 2018.

[33] R. V. Rao and D. P. Rai, "Optimisation of welding processes using quasi-oppositional-based Jaya algorithm," *Journal of Experimental & Theoretical Artificial Intelligence*, vol. 29, no. 5, Article ID 0952813, pp. 1099–1117, 2017.

[34] R. V. Rao, K. C. More, L. S. Coelho, and V. C. Mariani, "Multi-objective optimization of the Stirling heat engine through self-adaptive Jaya algorithm," *Journal of Renewable and Sustainable Energy*, vol. 9, no. 3, p. 033703, 2017.

[35] R. V. Rao and G. G. Waghmare, "A new optimization algorithm for solving complex constrained design optimization problems," *Engineering Optimization*, vol. 49, no. 1, pp. 60–83, 2017.

[36] N. Otsu, "A threshold selection method from gray-level histograms," *IEEE Transactions on Systems, Man, and Cybernetics*, vol. 9, no. 1, pp. 62–66, 1979.

[37] K. Kamalanand and P. M. Jawahar, "Comparison of swarm intelligence techniques for estimation of HIV-1 viral load," *IETE Technical Review*, vol. 32, no. 3, pp. 188–195, 2015.

[38] K. Kamalanand and P. Mannar Jawahar, "Comparison of particle swarm and bacterial foraging optimization algorithms for therapy planning in HIV/AIDS patients," *International Journal of Biomathematics*, vol. 9, no. 2, 1650024, 10 pages, 2016.

[39] V. Rajinikanth, N. S. MadhavaRaja, S. C. Satapathy, and S. L. Fernandes, "Otsu's multi-thresholding and active contour snake model to segment dermoscopy images," *Journal of Medical Imaging and Health Informatics*, vol. 7, no. 8, pp. 1837–1840, 2017.

[40] S. C. Satapathy, N. S. M. Raja, and V. Rajinikanth, "Multi-level image thresholding using Otsu and chaotic bat algorithm," *Neural Computing and Applications*, vol. 29, no. 12, pp. 1285–1307, 2018.

[41] G. H. Sudhan, R. G. Aravind, K. Gowri, and V. Rajinikanth, "Optic disc segmentation based on Otsu's thresholding and level set," in *Proceedings of the 2017 International Conference on Computer Communication and Informatics (ICCCI)*, pp. 1–5, Coimbatore, January 2017.

[42] "Brain Tumor Database (CEREBRIX and BRAINIX)," http://www.osirix-viewer.com/datasets/.

[43] N. Dey, V. Rajinikanth, A. S. Ashour, and J. M. R. S. Tavares, "Social group optimization supported segmentation and evaluation of skin melanoma images," *Symmetry*, vol. 10, no. 2, 2018.

[44] Z. Li, N. Dey, A. S. Ashour et al., "Convolutional neural network based clustering and manifold learning method for diabetic plantar pressure imaging dataset," *Journal of Medical Imaging and Health Informatics*, vol. 7, no. 3, pp. 639–651, 2017.

[45] K. Manickavasagam, S. Sutha, and K. Kamalanand, "Development of systems for classification of different plasmodium species in thin blood smear microscopic images," *Journal of Advanced Microscopy Research*, vol. 9, no. 2, pp. 86–92, 2014.

[46] A. Namburu, S. K. Samay, and S. R. Edara, "Soft fuzzy rough set-based MR brain image segmentation," *Applied Soft Computing*, vol. 54, pp. 456–466, 2017.

[47] R. F. Moghaddam and M. Cheriet, "A multi-scale framework for adaptive binarization of degraded document images," *Pattern Recognition*, vol. 43, no. 6, pp. 2186–2198, 2010.

[48] "Brats (Brain Tumor Database (BraTS-MICCAI))," http://hal.inria.fr/hal-00935640.

[49] K. S. Manic, I. S. Al Naimi, F. N. Hasoon, and V. Rajinikanth, "Jaya algorithm-assisted evaluation of tooth elements using digital bitewing radiography images," in *Computational Techniques*

for Dental Image Analysis, Advances in Medical Technologies and Clinical Practice, pp. 107–128, IGI Global, 2019.

[50] Y. Wang, Y. Chen, N. Yang et al., "Classification of mice hepatic granuloma microscopic images based on a deep convolutional neural network," *Applied Soft Computing*, vol. 74, pp. 40–50, 2019.

[51] A. Bakiya, K. Kamalanand, V. Rajinikanth, R. S. Nayak, and S. Kadry, "Deep neural network assisted diagnosis of time-frequency transformed electromyograms," *Multimedia Tools and Applications*, pp. 1–17, 2018.